T-lymphoid, megakaryocyte, and granulocyte development are sensitive to decreases in CBFβ dosage

Laleh Talebian,[1] Zhe Li,[1] Yalin Guo,[1] Justin Gaudet,[1] Maren E. Speck,[1] Daisuke Sugiyama,[1] Prabhjot Kaur,[2] Warren S. Pear,[3] Ivan Maillard,[4] and Nancy A. Speck[1]

[1]Department of Biochemistry, Dartmouth Medical School, Hanover, NH; [2]Department of Pathology, Dartmouth Medical School, Hanover, NH; [3]Department of Pathology & Laboratory Medicine, Abramson Family Cancer Research Institute, Institute for Medicine & Engineering, University of Pennsylvania, Philadelphia, PA; and [4]Division of Hematology-Oncology, University of Pennsylvania School of Medicine, Philadelphia, PA

The family of core-binding factors includes the DNA-binding subunits Runx1-3 and their common non–DNA-binding partner CBFβ. We examined the collective role of core-binding factors in hematopoiesis with a hypomorphic *Cbfb* allelic series. Reducing CBFβ levels by 3- or 6-fold caused abnormalities in bone development, megakaryocytes, granulocytes, and T cells. T-cell development was very sensitive to an incremental reduction of CBFβ levels: mature thymocytes were decreased in number upon a 3-fold reduction in CBFβ levels, and were virtually absent when CBFβ levels were 6-fold lower. Partially penetrant consecutive differentiation blocks were found among early T-lineage progenitors within the CD4$^-$CD8$^-$ double-negative 1 and downstream double-negative 2 thymocyte subsets. Our data define a critical CBFβ threshold for normal T-cell development, and situate an essential role for core-binding factors during the earliest stages of T-cell development. (Blood. 2007;109: 11-21)

Introduction

Hypomorphic alleles have long been known to cause developmental disorders in model organisms and in humans, and can reveal additional functions for genes in pathways that are completely obliterated when the gene's function is eliminated. For example, the many different spontaneous, chemically induced, and targeted mutant alleles of the *Kit* gene have illuminated c-kit's multiple roles in gametogenesis, melanogenesis, and hematopoiesis, and in the interstitial cells of Cajal.[1-3] Hypomorphic alleles can reveal differences in the requirements of certain developmental pathways for a protein's concentration, and help pinpoint lineage decisions that are influenced by that protein. Many mutations in cancer-causing genes may cause a functional dosage reduction as part of their overall activity, and the study of hypomorphic alleles may allow an assessment of this contribution.

In this study, we used a hypomorphic allele of the core-binding factor β *(Cbfb)* gene to unveil new developmental requirements for all 3 core-binding factors. Core-binding factors (CBFs) are a small family of transcription factors consisting of a DNA-binding subunit encoded by the *Runx1, Runx2,* or *Runx3* genes, and a common non–DNA-binding CBFβ subunit. Runx1 is required for hematopoietic stem cell (HSC) emergence in the fetus,[4] and during postnatal hematopoiesis for megakaryocyte, B-, and T-lymphocyte development.[5-7] Runx1 participates in CD4 silencing during the CD4$^-$CD8$^-$ double-negative (DN) and CD8$^+$ stages of T-cell development and is necessary at the DN2 to DN3 and DN3 to DN4 transitions.[5-8] Runx2 is required for bone formation, both for osteoblast differentiation and chondrocyte hypertrophy.[9-12] Runx3 contributes to the maturation of chondrocytes during bone formation[13] and is necessary for CD4 silencing at the CD8$^+$ stage of T-cell development, for Langerhans-cell development, and its deletion accelerates the maturation of dendritic cells resulting in an allergic airway inflammation.[7,8,14]

We used a hypomorphic *Cbfb* allele in conjunction with a nonfunctional *Cbfb* allele to create an allelic series. Reducing CBFβ levels should affect the activity of all 3 Runx proteins and reveal developmental requirements for the CBFs that were not previously uncovered with mutations in the individual Runx genes because of functional redundancy. Animals with 30% and 15% of wild-type CBFβ levels bypass the midgestation lethality and block in hematopoietic stem cell emergence suffered by *Cbfb*-deficient mice,[15,16] but die at birth with later developmental defects in both hematopoiesis and bone formation. In this paper, we describe the overall phenotype of mice with reduced CBFβ dosage, with an emphasis on T-cell development. We demonstrate that megakaryocyte, granulocyte, T-cell, and bone development are sensitive to reductions in CBFβ dosage to 30% and 15% of wild-type levels, but that B-cell and erythrocyte development are relatively unperturbed. A drop from 30% to 15% of wild-type CBFβ levels causes abrupt changes in both bone and T-cell development, identifying important concentration thresholds for CBFβ in these 2 processes.

Materials and methods

Cbfb alleles

The targeting vector for the *Cbfb^{rss}* allele contained a 4.2-kb *Sal*I-*Xho*I fragment from *Cbfb* intron 3 and a 5.3-kb *Avr*II-*Avr*II fragment from intron 4 as the 5′ and 3′ homology regions, respectively. We introduced a *Sac*II restriction site into a *Xho*I-*Avr*II genomic fragment containing exon 4 in pBluescript SK+ (Stratagene, La Jolla, CA) using the Quick-Change

Submitted May 3, 2006; accepted August 9, 2006. Prepublished online as *Blood* First Edition Paper, August 29, 2006; DOI 10.1182/blood-2006-05-021188.

The publication costs of this article were defrayed in part by page charge payment. Therefore, and solely to indicate this fact, this article is hereby marked "advertisement" in accordance with 18 USC section 1734.

mutagenesis kit (Stratagene) (upper strand primer, 5′-CTT GAA GGC TCC CGC GGT TCT GAA TGG AGT G-3′; lower strand primer, 5′-CAC TCC ATT CAG AAC CGC GGG AGC CTT CAA G-3′). We polymerase chain reaction (PCR) amplified the *lacZ* coding sequence together with the polyadenylation and cleavage site from pSV-β-galactosidase (Promega, Madison, WI) and subcloned it into pBluescript SK+ to make pSK-LacZ. A *Sac*II fragment containing the *lacZ* coding region and poly(A) sequence was then isolated from pSK-LacZ and inserted into the *Sac*II site that we had introduced into exon 4, in-frame with CBFβ protein coding sequences. The *Xho*I-*Avr*II fragment containing exon 4–*lacZ* was then inserted into the targeting vector just upstream of the normal exon 4, but in the reverse orientation (Figure 1A). The floxed-*neo* gene was introduced between the 5′ homologous region and exon 4–lacZ. A recombination signal sequence (RSS) for V(D)J recombination in the immunoglobulin and T-cell receptor loci with a 12-bp spacer (RSS12, 5′-CACAGTG CTACAGACTGGA ACAAAAAACC-3′) was inserted between floxed-*neo* and exon 4–lacZ, and RSS with a 23-bp spacer (RSS23, 5′-CACAGTG GTAGTACTCCACT-GTCTGGCTGT ACAAAAACC-3′) was introduced between the normal copy of exon 4 and the 3′ homology region. The *TK* gene was inserted upstream of the 5′ homologous region. The targeting vector was linearized with *Not*I and electroporated into J1 ES cells, and $Cbfb^{rss(neo)/+}$ mice were generated and screened by standard protocols. *Neo* was excised by crossing to *Tg(CMV-Cre)* mice to generate $Cbfb^{rss/+}$ mice, which were identified by Southern blot using the 5′ probe and an *Xba*I digest.

$Cbfb^{+/-}$ ($Cbfb^{tm1Spe/+}$) mice were described previously.[16] $Cbfb^{+/+}$, $Cbfb^{rss/+}$, and $Cbfb^{rss/rss}$ genotypes were determined by PCR using primers within exon 4 (5′-CTT GAA GGC TCC CAT GAT TCT G-3′) and intron 4 (5′-GCA GTT AAG AGC ACT GGT TGC C-3′) that amplify a 520-bp fragment from the wild-type allele and a larger 580-bp fragment from the $Cbfb^{rss}$ allele.

All mouse procedures were approved by Dartmouth College's Institutional and Animal Care Use Committee.

Skeletal preparations and histology

Skeletal preparations and histology were performed as described elsewhere.[17] The image in Figure 4A was acquired using a Nikon OPT1P HOT-O (Nikon, Tokyo, Japan) microscope equipped with a 10×/0.25 NA lens. Figure 4B was acquired with a Nikon C-SHG inverted microscope with a 10×/0.17 NA objective lens. Figure 4E was photographed in PBS with a Leica MZ FLIII stereomicroscope equipped with a Plan 1× (0.025–0.125 NA) objective lens (Leica, Heer Brugg, Switzerland). Figure 4F was acquired with a Nikon OPT1P HOT-O 40×/1.0 NA oil objective lens. Photographs were taken with a SPOT digital camera and SPOT Advance Software version 4.0 (Diagnostic Instruments, Sterling Heights, MI) and were processed with Adobe Photoshop 7.0 (Adobe Systems, San Jose, CA).

Western blot analysis

$CD45^+$ cells (clone 30-F11; BD Biosciences, San Jose, CA) were enriched from 17.5-dpc FLs by immunomagnetic selection using a magnetic-activated cell sorting (MACS) column following the manufacturer's instructions (Miltenyi Biotech, Auburn, CA). Cells (1×10^5 per mL) were resuspended in lysis buffer (150 mM NaCl, 50 mM Tris, pH 8.0, 1% nonidet P-40, 0.5% deoxycholate, 0.1% SDS, 0.2 mM EDTA, 2.0 mM EGTA plus 1 μg/mL pepstatin A, 1 μM Pefablock, 2 μg/mL leupeptin, 2 μg/mL aprotinin), lysates were boiled in SDS loading buffer and resolved by sodium dodecyl sulfate–polyacrylamide gel electrophoresis (SDS-PAGE) through 13% gels, and the proteins were transferred to nitrocellulose. The nitrocellulose was cut into 2 pieces between the 25.9- and 37.1-kDa markers, the top half of the membrane was probed with an antibody to mouse actin (20-33; Sigma, St Louis, MO) and the bottom half was probed with a mouse monoclonal antibody to CBFβ (β141.2),[16] and the blots were developed with enhanced chemiluminescence (ECL) reagents (Amersham, Arlington Heights, IL). Western blot quantification of endogenous CBFβ was performed by comparison to known amounts of bacterially produced and purified CBFβ(1-141). Actin and CBFβ were quantified by densitometry and analyzed using ImageQuant 5 (Molecular Dynamics, Sunnyvale, CA).

RT-PCR

RT-PCR on RNA prepared from 17.5-dpc FLs was performed using Qiagen Omniscript RT kit (Qiagen, Valencia, CA) with one primer from exon 1 of the *Cbfb* gene (5′-AGACGGATCC**ATG**CCGCGCGTCGTCCCGGAC-3′, a *Bam*HI site [underlined] was incorporated immediately 5′ to the initiating ATG [bold]) and a second primer downstream of a *Pst*I site in exon 6 (5′-GTTAAGCAACCCTGATAC-3′). The *Hprt* gene was amplified with the following primers: 5′-CACAGGACTAGAACAGGTGC-3′ and 5′-GCTGGTGAAAAGGACCTCT-3′. The *Cbfb* RT-PCR products were digested with *Bam*HI and *Pst*I, subcloned into pBluescript SK+ (Stratagene), and sequenced.

Real-time PCR

$Gr\text{-}1^+$ cells were enriched from 17.5-dpc $Cbfb^{+/+}$ and $Cbfb^{rss/-}$ FLs by immunomagnetic selection using a MACS column. Total RNA was harvested using Qiagen's RNeasy Mini Kit. Double-stranded cDNA for real-time quantitative PCR (RTQ-PCR) was generated from 2 to 5 μg total RNA using the Superscript II double-strand cDNA synthesis kit (Invitrogen) according to the manufacturer's instructions. cDNA was then quantified using a NanoDrop (NanoDrop Technologies, Wilmington, DE). SYBR Green (Applied Biosystems, Foster City, CA) RTQ-PCR was used to measure transcript abundance in each sample. RTQ-PCR assays were performed in triplicate for each sample on Applied Biosystems' ABI 7500. Primers for each gene were designed using Primer Express v2.0 software (Applied Biosystems) and are as follows: *Csf3r* (GCSFR) fwd, 5′-ATCATCAAGGGCAGGACATACA-3′ and rev, 5′-AGGCCACAAGGGT-CACGTT-3′; *Csr1r* (MCSFR) fwd, 5′-CATGGCCTTCCTTGCTTCTAA-3′ and rev, 5′-ACATGTCCGCTGGTCAACAG-3′; *Mpo* fwd, 5′-ATCACGGC-CTCCCAGGATAC-3′ and rev, 5′-TGCCAACTCCAGGTTCTTCAG-3′; *Ela2* fwd, 5′-AGGAGGCTGTGGATCTGGATT-3′ and rev, 5′-TGCCTTCGGATA-ATGGAATTG-3′; *Pu.1* fwd, 5′-TCCTACATGCCCCGGATGT-3′ and rev, 5′-TCTCACCCTCCTCCTCATCTGA-3′; *Cebpa* fwd, 5′-GAGCCGAGATA-AAGCCAAACA-3′ and rev, 5′-AGGCAGCTGGCGGAAGAT-3′; *Cebpe* fwd, 5′-AGTACCGACTGCGACGTGAAC-3′ and rev, 5′-GACCTTCTGCT-GAGTCTCCATAATG-3′; *Mmp9* (*Gelatinase* B) fwd, 5′-GGACGACGT-GGGCTACGT-3′ and rev, 5′-CTGCACGGTTGAAGCAAAGA-3′; *Lct* fwd, 5′-CCTGCACACTTGGACTTGCTT-3′ and rev, 5′-GACAGAAACAT-CACGTGGTTGTC′; and *Gapdh* fwd, 5′-CATGGCCTTCCGTGTTCCTA-3′ and rev, 5′-TGTCATCATACTTGGCAGGTTTCT-3′.

Progenitor assays

Single-cell suspensions of FL cells were prepared in 1 to 3 mL alpha minimal essential medium (Gibco, Grand Island, NY) by grinding and passing the tissue through a sterile 70-μm filter. CFU-GEMM, CFU-GM, and BFU-E progenitors from 12.5-dpc fetuses were enumerated by culturing 1/20th of each liver in 3 mL methylcellulose medium (MethoCult GF M3434) containing stem-cell factor (SCF), interleukins 3 and 6, and erythropoietin following the manufacturer's instructions (Stem Cell Technologies, Vancouver, BC, Canada). For 15.5- to 17.5-dpc fetuses, 5×10^5 FL cells were cultured. Colonies were scored and counted 7 to 9 days after culture. Megakaryocyte progenitors were enumerated using the Megacult-C kit (Stem Cells Technologies) by plating 2.2×10^5 17.5-dpc FL cells per 2-chambered slide (plus thrombopoietin, IL-6, and IL-3) and counting 8 to 10 days later.

Clinical blood counts

Peripheral blood was collected with heparinized capillary tubes (Fisher, Hampton, NH) into blood-collection tubes (Sarstedt, Nümbrecht, Germany), diluted 1:1 with FBS, and counted on a Hemavet 950 blood analyzer (HV 950 FS; Drew Scientific, Orford, CT).

In vitro differentiation of megakaryocytes and platelets from fetal liver

In vitro cultures were performed as described by Shivdasani et al.[18] Livers from 13.5-dpc fetuses were removed and transferred to a falcon tube containing DMEM/10% FCS, and the cells were dispersed by passage 3

times each through 18-, 21-, and 25-gauge needles. The cells were collected by centrifugation at room temperature at 320*g* for 3 minutes, and resuspended in 1 mL DMEM/10% FCS. Thrombopoietin was added to a final concentration of 50 ng/mL, and cells were cultured for 3 days at 37°C. The cultured cells were harvested by centrifugation, resuspended in 1.0 mL DMEM/10% FCS, layered onto a discontinuous BSA gradient containing 2 mL 3% BSA (in PBS) and 1 mL 1.5% BSA in a 15-mL conical tube, and left undisturbed for 30 to 40 minutes at room temperature. The supernatant was aspirated, and the cell pellet was washed, resuspended in 3 mL DMEM/10% FCS, and cultured for 48 hours at 37°C. The culture was collected and centrifuged at 200*g* at room temperature for 5 minutes and the supernatant centrifuged at 2500*g* at room temperature for an additional 10 minutes. The platelet pellet was resuspended in 200 μL PBS, stained with FITC-conjugated CD41 antibody (BD Biosciences), and analyzed by flow cytometry.

Flow cytometry

Cell-surface antigens were detected by immunofluorescence assays using one or a combination of PE, FITC, APC, PerCp, APC-Cy7, PE-Cy7, Pacific Blue, and PerCp-Cy5.5 fluorochromes and the following monoclonal antibodies: CD19 (1D3), B220 (RA3-6B2), Gr-1 (RB6-8C5), Mac1 (M1/70), c-kit (2B8), CD45 (30-F11), CD4 (RM4-5), CD8α (53-6.7), CD3ϵ (145-2C11), CD44 (IM7), CD25 (7D4 or PC61), IL7Rα (A7R34), TCRβ (H57-597), TCRγδ (GL3), Ter119 (TER-119), Thy1.2 (30-H12), CD11c (HL3), Sca-1 (E13-161.7), CD41 (MWReg30), NK1.1 (PK136), Ly5.1 (A20), and Ly5.2 (104) (Pharmingen, San Diego, CA; and Ebiosciences, San Diego, CA). The following cocktail omitting CD4 was used to exclude Lin^+ cells in the thymus: CD19, B220, Gr-1, Mac1, CD8α, CD3ϵ, TCRβ, TCRγδ, Ter119, CD11c, and NK1.1. Fluorescence-activated cell sorting (FACS) analysis was performed using a FACScan or FACSCalibur (BD Biosciences). For BM, thymus, and spleen of animals that underwent transplantation, analytic flow cytometry was performed on a 4-laser LSR II (BD Biosciences). Doublets were excluded using forward scatter (FSC) area versus width pulses. 4,6-diamidino-2-phenylindole (DAPI) was used to exclude dead cells. The resulting files were uploaded into FlowJo (Tree Star, San Carlos, CA) for analysis.

Transplant analyses

C57BL/6 (B6.SJL-Ptprc<a>Pep3<b>/BoyJ) × 129S1/SVImJ F1 mice ($Ly5.1^+/Ly5.2^+$) were subjected to 2 split doses of 5.5 Gray 3 to 4 hours apart. Each recipient received donor FL and competitor BM cells (2×10^5 cells of each) via tail-vein injection. All donor fetuses were of a mixed C57BL/6J and 129S1/SVImJ background and expressed the Ly5.2 (CD45.2) haplotype. Whole BM competitor cells were prepared from C57BL/6 (B6.SJL-Ptprc<a>Pep3<b>/BoyJ) ($Ly5.1^+$) mice.

Peripheral blood of transplant recipients was collected in K3EDTA-coated vacutainer tubes (Sarstedt) and mixed immediately on a roller at room temperature. FACS Lysis Solution (BD Biosciences) was added and samples were stained with cell-surface markers as per the manufacturer's protocol. Staining of BM, thymus, and spleen of the animals that underwent transplantation was performed in PBS/3% FCS after blocking with 2.4G2 (anti-FcγII/IIIR) hybridoma supernatant and rat/mouse IgG (Sigma).

Results

The hypomorphic *Cbfb^{rss}* allele

We attempted to modify the *Cbfb* locus so that the RAG1/RAG2 recombinases would rearrange and selectively inactivate the gene during B- and T-lymphocyte development, and at the same time mark the cells in which the rearrangement had occurred. To this end, we introduced the *lacZ* gene and recombination signal sequences (RSS) into the third intron of *Cbfb,* creating what we called the *Cbfb^{rss}* allele (Figure 1). However, mice homozygous for the *Cbfb^{rss}* allele died at birth from causes apparently unrelated to impaired lymphopoiesis, as will be described below (see the next section and Figure 2).

We could find no evidence for β-galactosidase expression or rearrangement of the *Cbfb^{rss}* allele in lymphocytes (not shown). Instead, the exogenous sequences in the mutant allele altered splicing. Specifically, more than half of the mRNA from the *Cbfb^{rss}* allele lacked exon 4, and properly spliced mRNA was present at lower than normal amounts (Figure 1C). Exon 4 encodes amino acids 95 to 133, which encompass the C-terminal one third of the heterodimerization domain for the Runx proteins. The predicted molecular weight of CBFβΔ95-133 is 17.5 kDa, but we could find no evidence of this protein in cells (Figure 1D). Instead full-length CBFβ was present, but in reduced amounts. Hence *Cbfb^{rss}* is a hypomorphic *Cbfb* allele from which lower-than-normal amounts of full-length CBFβ protein are produced.

To further reduce CBFβ protein levels, we crossed *Cbfb$^{rss/+}$* mice to *Cbfb$^{+/-}$ (Cbfb$^{+/tm1Spe}$)* mice. The *Cbfb^{tm1Spe}* allele contains a deletion of exon 5. No full-length CBFβ protein is produced in *Cbfb$^{-/-}$* fetuses, and a truncated protein is undetectable.[16] Through a combination of *Cbfb$^{rss/+}$* intercrosses and *Cbfb$^{rss/+}$* × *Cbfb$^{+/-}$* matings, we created an allelic *Cbfb* series, in which we reduced the levels of full-length CBFβ protein to approximately 65% *(Cbfb$^{rss/+}$),* 50% *(Cbfb$^{+/-}$),* 30% *(Cbfb$^{rss/rss}$),* and 15% *(Cbfb$^{rss/-}$)* of wild-type protein levels (Figure 1D).

Reduced CBFβ dosage impairs bone ossification

Cbfb$^{rss/rss}$ and *Cbfb$^{rss/-}$* mice were born at normal Mendelian ratios (not shown), but died at postnatal day 0, the same time at which Runx2-deficient mice were reported to die.[9,10] Newborn *Cbfb$^{rss/rss}$* mice had defects in skeletal formation, including delays in the ossification of ribs, metacarpals/metatarsals, phalanges, pelvis, sternum, and vertebrae, and exhibited hypoplastic clavicles, scapulas, calvaria, maxillas, and mandible (Figure 2A). Long bones from *Cbfb$^{rss/rss}$* fetuses showed reduced primary ossification of the diaphysis and delayed appearance of secondary ossification centers (Figure 2B). The further 2-fold reduction of CBFβ levels in *Cbfb$^{rss/-}$* fetuses greatly increased the severity of skeletal defects. Sections through the tibia revealed essentially no alkaline phosphatase–positive osteoblasts in either the diaphysis or bone collar, and although hypertrophic chondrocytes were present, they were alkaline phosphatase negative (Figure 2B). These data define 2 critical thresholds for CBFβ protein concentration in bone development at which skeletal formation is moderately (30% CBFβ) and severely (15% CBFβ) impaired. The cause of neonatal death is not known, but the skeletal and cranial defects could potentially affect either or both respiration and nursing. We saw no evidence of hemorrhaging, and CBCs on peripheral blood of 18.5-dpc fetuses revealed normal red blood cell counts and hemoglobin content (Table 1).

CBFβ dosage affects megakaryocyte development and/or maturation

Fetal livers from 12.5-dpc *Cbfb$^{rss/-}$* animals contained approximately half the number of granulocyte-macrophage units (CFU-GM) and burst-forming units–erythroid (BFU-Es) than other *Cbfb* genotypes (Figure 3A). This trend was reversed at 17.5 days after coitus, at which point *Cbfb$^{rss/rss}$* and *Cbfb$^{rss/-}$* fetal livers contained more CFU-Cs (Figure 3B) and megakaryocyte progenitors (CFU-Mks) (Figure 3C) than their littermates. CFU-C assays at intermediate time points revealed that the gestational age at which fetal liver progenitors began to accumulate was 15.5 days after coitus

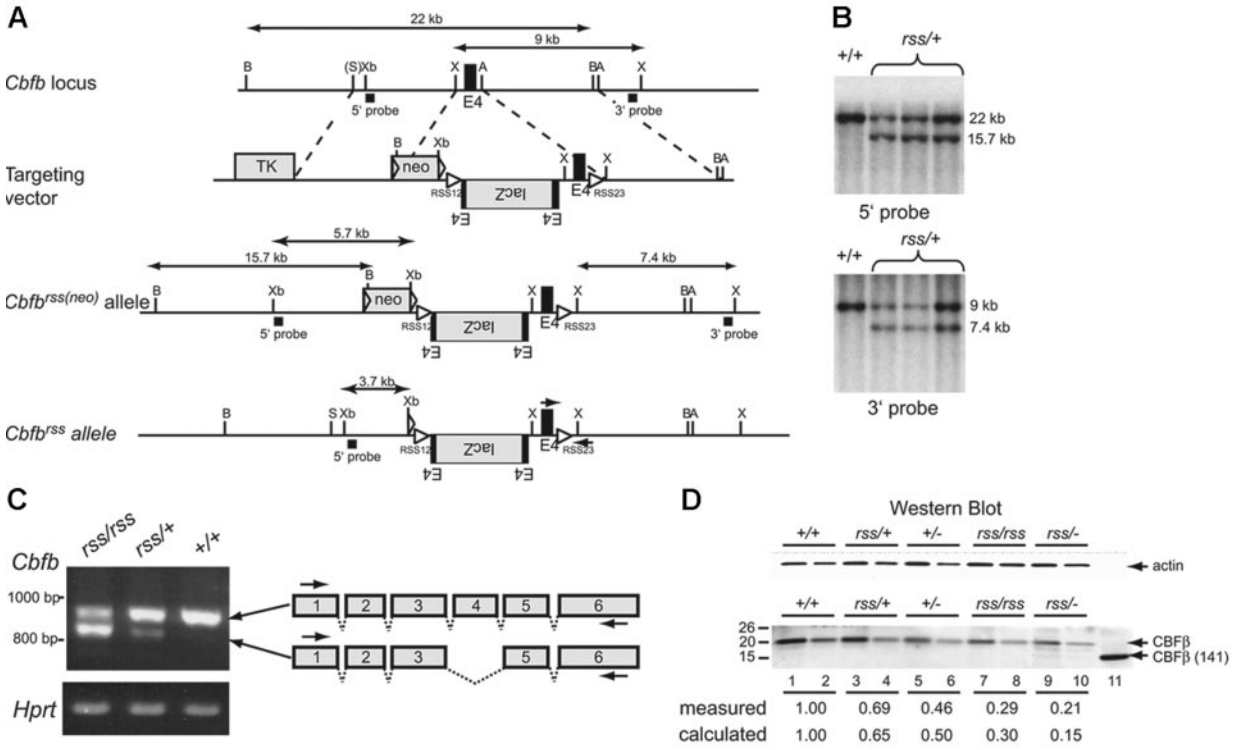

Figure 1. The hypomorphic *Cbfb^{rss}* allele. (A) Targeting vector, targeted *Cbfb$^{rss(neo)}$* locus, and the *Cbfb^{rss}* allele following excision of floxed *neo* by *Tg(CMV-Cre)*. The *Cbfb^{rss}* allele contains the *lacZ* gene in the reverse orientation flanked by an extra copy of exon 4, inserted into intron 3. The targeting vector also contains a recombination signal sequence (RSS12) in intron 3, and the RSS23 sequence in intron 4. *Cbfb* exons are black, introduced coding sequences (*lacZ,* floxed-*neo, TK*) are gray, and both the loxP sequences flanking *neo* and the RSS sequences are indicated by triangles. The expected sizes of the *Xho*I restriction fragments that hybridize with the 3′ probe and the *Bam*HI and *Xba*I fragments that hybridize with the 5′ probe are indicated. PCR primers for genotyping are indicated by arrows on the *Cbfb^{rss}* allele. A indicates *Avr*II; B, *Bam*HI; X, *Xho*I; S, *Sal*I; and Xb, *Xba*I. (B) Southern blots showing correct targeting (prior to *neo* excision) at both the 5′ and 3′ ends. Top shows *Bam*HI digest; bottom, *Xho*I digest. (C) RT-PCR showing the 2 predominant mRNAs generated from the *Cbfb^{rss}* allele. The top band contains all 6 *Cbfb* exons and encodes a 22-kDa protein, while the bottom band lacks exon 4 and encodes a 17.5-kDa protein. RT-PCR for *Hprt* was used as a loading control. Arrows on the schematic diagram show the location of RT-PCR primers. (D) Western blot of lysates prepared from CD45$^+$ cells isolated from 17.5-dpc FLs probed for actin (top) and CBFβ (bottom). Lysate from 4×10^4 *Cbfb$^{+/+}$* cells was loaded in lane 1. The amount of *Cbfb$^{rss/+}$*, *Cbfb$^{+/-}$*, *Cbfb$^{rss/rss}$*, and *Cbfb$^{rss/-}$* lysates loaded in lanes 3, 5, 7, and 9 was adjusted based on the actin signal. Lanes 2, 4, 6, 8, and 10 are 2-fold dilutions of each lysate. The 22-kDa endogenous CBFβ protein, and the purified heterodimerization domain CBFβ (141) used as a blotting control are indicated with arrows. The measured amount of CBFβ in each sample was normalized relative to actin, and is expressed relative to *Cbfb$^{+/+}$* cells (averaged from 2-4 experiments) below the lanes. The calculated amount is based on the observation that approximately one third of the mRNA produced from the *Cbfb^{rss}* allele is properly spliced. Wild-type CD45$^+$ cells contain 2.4×10^5 CBFβ molecules/cell as determined by comparison with dilutions of the CBFβ (141) standard (not shown).

(not shown). Similar phenomena of reduced numbers of CFU-Cs at midgestation (12.5 days after coitus) and increased numbers in adult bone marrow were reported in mice haploinsufficient for Runx1.[16,19] The mechanism underlying either effect is poorly understood.[4,19]

Megakaryocyte colonies derived from cultures of *Cbfb$^{rss/-}$* 17.5-dpc fetal livers were denser and contained smaller, more uniform-sized cells (not shown) with reduced acetylcholinesterase (brown) staining (Figure 4A). Megakaryocytes were visible 48 hours after 13.5-dpc *Cbfb$^{+/+}$* fetal liver (FL) cells were cultured in the presence of thrombopoietin, but no large megakaryocytes were seen in cultures from *Cbfb$^{rss/-}$* cells (Figure 4B), and fewer platelets were generated (Figure 4C-D). Peripheral blood from 18.5-dpc *Cbfb$^{rss/-}$* fetuses had a tendency toward fewer platelets,

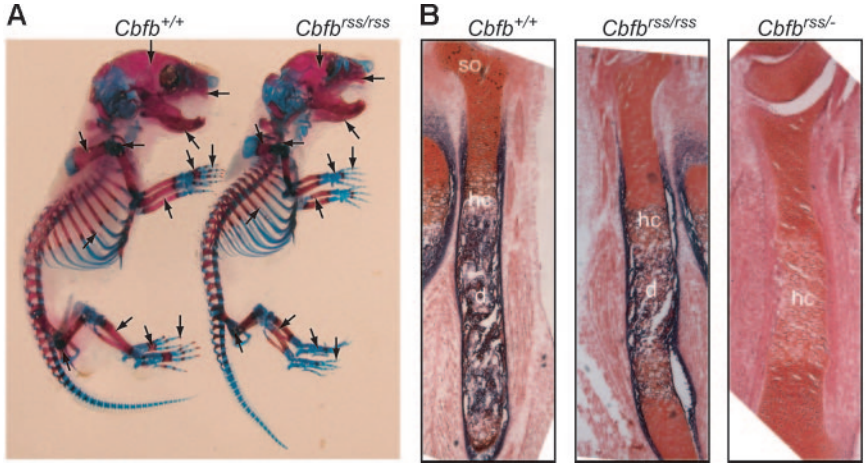

Figure 2. Bone defects in *Cbfb$^{rss/rss}$* and *Cbfb$^{rss/-}$* fetuses. (A) Alcian blue– and alizarin red–stained skeletal preparations from postnatal day 0.5 *Cbfb$^{+/+}$* and *Cbfb$^{rss/rss}$* fetuses. Cartilaginous skeleton is blue and ossified bone is pink. Areas of skeletal abnormalities are indicated with arrows. (B) Tibias from 17.5-dpc *Cbfb$^{+/+}$*, *Cbfb$^{rss/rss}$*, and *Cbfb$^{rss/-}$* fetuses stained for cartilage with safranin O (red) and for osteoblasts and hypertrophic chondrocytes by virtue of their alkaline phosphatase activity (blue). hc indicates hypertrophic chondrocytes; d, diaphysis; and so, secondary ossification center.

Table 1. Clinical blood counts from 18.5-dpc fetuses

Parameter	+/+	rss$^{-/-}$
RBCs, × 10^{12}/L	1.8 ± 0.5	2.2 ± 0.8
Hb, g/L	60 ± 15	78 ± 23
MCV, fL	139.8 ± 5.4	151.3 ± 12.5
PLTs, K/10^9/L	260.3 ± 58.3	222.0 ± 70.3

Clinical blood counts from *Cbfb*$^{+/+}$ (n = 6) and *Cbfb*$^{rss/-}$ (n = 5) fetuses. Averages (± SD) are indicated. No parameters were significantly different.

although the difference was not significant (Table 1). The relatively high variability in platelet counts among fetuses may contribute to the lack of significance. Runx1 is required for megakaryocyte development,[5,6,19] and haploinsufficiency of RUNX1 causes a familial platelet disorder in humans.[20] Our data suggest that CBFβ may be required for Runx1 function in megakaryocyte differentiation, although this effect was observed only in vitro. The in vitro data are consistent, though, with those of Kuo et al who showed that a conditionally activated dominant-negative *CBFB/MYH11* allele impaired megakaryocyte differentiation.[21]

Granulocyte development is sensitive to CBFβ dosage

We observed subtle reductions in the size and cellularity of spleens from *Cbfb*$^{rss/rss}$ and *Cbfb*$^{rss/-}$ fetuses (Figure 4E; Table 2). The absolute number of CD45$^+$ cells per spleen was decreased 4- to 5-fold, and the total number of monocytes/granulocytes (Gr-1$^+$Mac-1$^+$) was 10- to 20-fold lower ($P < .001$). The percentages of CD19$^+$ B lymphocytes and Ter119$^+$ erythrocytes in *Cbfb*$^{rss/rss}$ and *Cbfb*$^{rss/-}$ spleens were unaltered, although the total numbers of CD19$^+$ and Ter119$^+$ cells were decreased 2.8-fold ($P < .05$), therefore we cannot rule out a moderate impairment in these lineages.

Cytospin preparations of Gr-1$^+$ cells enriched from 17.5-dpc *Cbfb*$^{+/+}$ fetal livers contained abundant segmented neutrophils and bands (Figure 4F). Preparations from *Cbfb*$^{rss/-}$ fetuses contained no segmented mature neutrophils and almost no bands, but many immature monocytoid cells were found. There was no significant decrease in the levels of mRNAs for either granulocyte-monocyte colony-stimulating factor receptor (GCSFR) or macrophage CSFR (MCSFR), or for the primary granule protein myeloperoxidase (Figure 4G), which is normally found beginning at the promyelocyte stage of granulocyte development and in monocytes. However, the mRNA for another primary granule protein, neutrophil elastase, which is also found beginning at the promyelocyte stage, and is a direct CBF target,[22,23] was significantly decreased, as was mRNA encoding the secondary and tertiary granule proteins, lactoferrin and gelatinase B. mRNA encoding C/EBPϵ, a transcription factor required for the expression of secondary and tertiary granule proteins,[24,25] was significantly lower, as was PU.1 mRNA. C/EBPα expression was not significantly changed, consistent with the unaltered expression of one of its targets, GCSFR.[26]

Fetal thymocytes are affected by reduced CBFβ dosage

The thymuses of *Cbfb*$^{rss/rss}$ and *Cbfb*$^{rss/-}$ fetuses were small (Figure 4E), and thymus cellularity was significantly decreased (Table 2). Thymuses from *Cbfb*$^{rss/rss}$ and *Cbfb*$^{rss/-}$ fetuses contained a significantly smaller percentage of CD4$^+$CD8$^+$ cells (Table 2), and the absolute number of CD4$^+$CD8$^+$ thymocytes was approximately 10-fold lower in *Cbfb*$^{rss/rss}$ fetuses and more than 100-fold lower in *Cbfb*$^{rss/-}$ fetuses ($P < .001$) (Figure 4H). Thymic B cells had been seen upon conditional inactivation of Notch1 in adult mice,[27,28] but we found no evidence of B-cell accumulation in 17.5-dpc *Cbfb*$^{rss/-}$ thymuses (not shown). The percentage of CD4$^+$ cells was increased in *Cbfb*$^{rss/rss}$ fetal thymuses (Figure 4I; Table 2) due to partial derepression of CD4 expression, which is normally silenced by Runx1 during the double-negative (DN) stages of thymocyte development.[7] Indeed, the CD4$^+$CD8$^-$ population in *Cbfb*$^{rss/rss}$ thymuses expressed low levels of TCRβ (Figure 4I), indicating that these were not bona fide mature CD4 SP cells, but rather were more immature thymocytes that had inappropriately up-regulated CD4 or failed to up-regulate CD8. The percentage of TCRβ$^+$ cells was decreased in the CD4$^+$CD8$^+$ thymocyte population of *Cbfb*$^{rss/rss}$ fetuses and the percentage of TCRγδ$^+$ thymocytes was also lower (Figure 4I).

Granulocyte and T-cell defects in *Cbfb*$^{rss/rss}$ and *Cbfb*$^{rss/-}$ mice are cell autonomous

We transplanted equal numbers of Ly5.2$^+$ fetal liver (FL) donor cells and Ly5.1$^+$ bone marrow (BM) competitor cells into irradiated Ly5.1$^+$/Ly5.2$^+$ mice and analyzed their contribution to peripheral blood 4 months later. Donor cells from *Cbfb*$^{+/+}$, *Cbfb*$^{rss/rss}$, and *Cbfb*$^{rss/-}$ FL all reconstituted hematopoiesis in recipient mice, and therefore contained functional HSCs (Figure 5A-D). Both *Cbfb*$^{rss/rss}$ and *Cbfb*$^{rss/-}$ FL cells contributed to Gr-1$^+$ and Mac-1$^+$ cells in peripheral blood, however there were differences in the FACS profiles of the donor-derived granulocytes (Figure 5A). Specifically, the donor-derived cells in recipients repopulated with either *Cbfb*$^{rss/rss}$ or *Cbfb*$^{rss/-}$ FL lacked a population of Gr-1^{hi}Mac-1^{lo} cells (R2 gate), and accumulated a population of Gr-1^{hi}Mac-1^{hi} cells (R3 gate). Cytospin preparations of purified Gr-1^{hi}Mac-1^{lo} cells from the R2 gate consisted almost entirely (≥ 98%) of segmented neutrophils, while 85% (± 6.7%) of the Gr-1^{hi}Mac-1^{hi} population (R3 gate) consisted of segmented neutrophils, of which a small number were bands (1.5%), and the remaining cells (14.5%) were monocytes (not shown). These data suggest that reduced CBFβ levels modestly perturb granulocyte

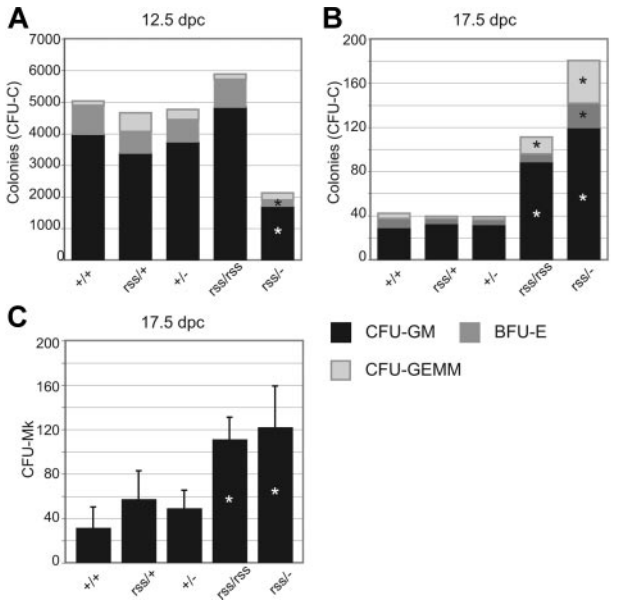

Figure 3. Effect of CBFβ dosage on hematopoietic progenitor numbers. (A) CFU-GMs, BFU-Es, and CFU-GEMMs in 12.5-dpc fetal livers. $n_{+/+} = 14$, $n_{rss/+} = 12$, $n_{+/-} = 11$, $n_{rss/rss} = 4$, and $n_{rss/-} = 4$. Asterisks indicate differences from *Cbfb*$^{+/+}$ significant at $P = .01$. (B) CFU-Cs per 5×10^5 17.5-dpc fetal liver cells. $n_{+/+} = 9$, $n_{rss/+} = 7$, $n_{+/-} = 9$, $n_{rss/rss} = 4$, and $n_{rss/-} = 8$. Asterisks indicate differences from *Cbfb*$^{+/+}$ significant at $P = .01$. (C) Megakaryocyte progenitors (CFU-Mk) per 2.2×10^5 17.5-dpc fetal liver cells. $n_{+/+} = 10$, $n_{rss/+} = 14$, $n_{+/-} = 11$, $n_{rss/rss} = 3$, and $n_{rss/-} = 6$. Asterisks indicate differences between *Cbfb*$^{rss/rss}$ and *Cbfb*$^{rss/-}$ versus all other genotypes significant at $P = .01$.

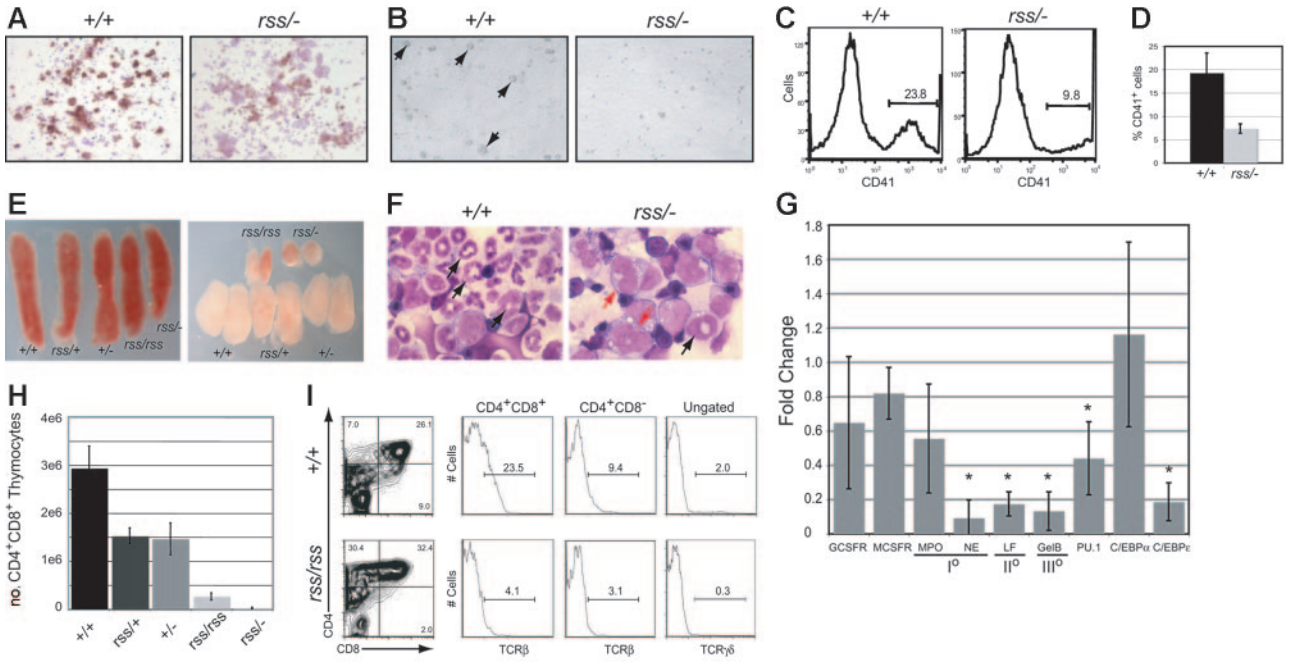

Figure 4. Megakaryocyte, granulocyte, and T-cell development in the fetus are sensitive to CBFβ dosage. (A) Morphology and acetylcholinesterase staining (brown) of megakaryocyte colonies from CFU-Mk assays. Note the reduced intensity of acetylcholinesterase staining in *Cbfb*$^{rss/-}$ megakaryocyte colonies, indicating impaired differentiation. (B) Megakaryocytes (large cells, arrows) were obtained following in vitro differentiation of 13.5-dpc fetal liver cells in liquid cultures in the presence of thrombopoietin. Note the absence of large cells in the *Cbfb*$^{rss/-}$ culture. (C) Histogram of CD41 expression in platelets isolated from in vitro megakaryocyte cultures. (D) Average percentage of CD41$^+$ platelets from megakaryocyte cultures. $n_{+/+} = 4$, $n_{rss/-} = 4$. Error bars represent 95% confidence intervals. The difference between *Cbfb*$^{+/+}$ and *Cbfb*$^{rss/-}$ cultures was significant at $P < .03$. (D) (E) Pictures of spleens (left panel) and thymic lobes (right panel) from 17.5-dpc fetuses. (F) Morphology of Gr-1$^+$ cells enriched from 17.5-dpc fetal livers. Arrows in *Cbfb*$^{+/+}$ panel point to mature and band neutrophils. Red arrows in the *Cbfb*$^{rss/-}$ sample indicate immature monocytoid cells, and the black arrow points to a rare band. (G) Real-time PCR for myeloid-specific gene expression in Gr-1$^+$ cells enriched from *Cbfb*$^{+/+}$ and *Cbfb*$^{rss/-}$ 17.5-dpc fetal livers. Gene-expression data are presented as the fold change in *Cbfb*$^{rss/-}$ cells relative to *Cbfb*$^{+/+}$ cells (normalized to a value of 1) and represent averages from 3 independent experiments. Error bars indicate 95% confidence intervals. For each sample, expression values were normalized to *Gapdh*. GCSFR indicates granulocyte colony-stimulating factor receptor; MCSFR, macrophage colony-stimulating factor receptor; MPO, myeloperoxidase; NE, neutrophil elastase; LF, lactoferrin; GelB, gelatinase B; and I°, II°, III°, primary, secondary, and tertiary, respectively, granule proteins. The asterisks indicate expression differences significant at $P < .001$. (H) Total number of CD4$^+$CD8$^+$ (DP) thymocytes in 17.5-dpc fetuses. Error bars represent standard errors. The differences between *Cbfb*$^{+/+}$ and all other genotypes were significant at $P < .001$. (I) CD4 expression is derepressed, and the percentage of TCRβ and γδ cells decreased in 17.5-dpc *Cbfb*$^{rss/rss}$ thymocytes. The 2 histograms on the left show the percentage of CD4$^+$CD8$^+$ (DP) cells and CD4$^+$CD8$^-$ thymocytes that are TCRβ$^+$. The histogram on the far right shows the percentage of total thymocytes that are TCRγδ$^+$. The average percentages of TCRβ$^+$ DP cells (± SD) are as follows: *Cbfb*$^{+/+}$, 20.1 (2.9), *Cbfb*$^{rss/rss}$, 5.6 (2.6); for percentages of TCRβ$^+$ CD4$^+$ cells: *Cbfb*$^{+/+}$, 19.8 (10.5), *Cbfb*$^{rss/rss}$, 5.1 (2.2); and for percentages of TCRδγ$^+$ cells: *Cbfb*$^{+/+}$, 1.9 (0.2), *Cbfb*$^{rss/rss}$, 0.4 (0.1).

development or the expression of granulocyte markers in a cell-autonomous manner. *Cbfb*$^{rss/rss}$ and *Cbfb*$^{rss/-}$ FL cells contributed to B220$^+$ B cells in the peripheral blood of mice that underwent transplantation (Figure 5A), consistent with the relatively normal numbers of B cells found in the 17.5-dpc fetal spleen. In contrast, the percentage of donor-derived Thy1.2$^+$ peripheral-blood T cells was moderately decreased in mice that received a transplant of *Cbfb*$^{rss/rss}$ FL cells, and Thy1.2$^+$, CD4$^+$, and CD8$^+$ cells were virtually absent in mice that received a transplant of *Cbfb*$^{rss/-}$ FL cells (Figure 5A).

Bone marrow at 12 months after transplantation was reconstituted almost exclusively from FL donor cells regardless of the *Cbfb* genotype, consistent with the greater proliferative capacity of FL HSCs.[29] More than 90% of c-kit$^+$Sca-1$^+$Lin$^-$ (KSL) cells in all recipient mice were donor derived (Figure 5B). The donor-derived KSL population was expanded approximately 2.5-fold in bone marrow reconstituted with *Cbfb*$^{rss/rss}$ or *Cbfb*$^{rss/-}$ FL cells (Figure 5B R2 gate, and Figure 5C), consistent with the observed increase of CFU-Cs in the 17.5-dpc fetal liver (Figure 3B) and with findings in *Runx1*$^{+/-}$ and conditional *Runx1* knock-out mice.[6,19]

The majority of Ter119$^+$ CD45$^+$ erythroid lineage cells in the bone marrow were donor derived (not shown), as were Gr-1$^+$Mac-1$^+$ cells (Figure 5D). However, whereas CD4$^+$CD8$^+$ thymocytes in recipients reconstituted with *Cbfb*$^{+/+}$ or *Cbfb*$^{rss/rss}$ FL cells were almost entirely donor derived, there were essentially no donor-derived CD4$^+$CD8$^+$ thymocytes in mice that received a transplant of *Cbfb*$^{rss/-}$ FL cells (Figure 5E), despite the overwhelming contribution of FL-derived cells to the bone marrow in the same recipients (Figure 5B-D). Therefore, there is an abrupt, profound, cell-autonomous loss of T-cell potential associated with a drop in CBFβ levels from 30% to 15% of normal.

CBFβ is required at the earliest stages of T-cell development

CD4$^+$CD8$^+$ double-positive (DP) thymocytes are derived from early T-lineage progenitors (ETPs) that likely differentiate from rare circulating BM-derived progenitors with a KSL phenotype that seed the thymus.[30,31] Since *Cbfb*$^{rss/-}$ FL cells did not contribute to the formation of CD4$^+$CD8$^+$ DP cells, we examined their contribution to the ETP and DN populations of thymocytes in transplant recipient mice to more precisely define the nature of the T-cell developmental block. The ETP, DN2, and DN3 populations in recipients that received a transplant of *Cbfb*$^{+/+}$ or *Cbfb*$^{rss/rss}$ FL cells were almost entirely derived from FL Ly5.2$^+$ donor cells (Figure 6A). In contrast, the contribution of *Cbfb*$^{rss/-}$ FL cells to the ETP, DN2, and DN3 populations was both less efficient and variable. In 6 of 9 recipient mice, exemplified by *rss/−* (1) (Figure 6A), there was essentially no FL Ly5.2$^+$ donor-cell contribution to DN2 or DN3 cells, despite the fact that more than 90% of these recipients' bone marrow was FL donor derived. This was indicative

Table 2. Decreased CBFβ dosage alters the percentage of monocytes/granulocytes and T cells in the spleen and thymus of 17.5-dpc fetuses

	Genotype									
	Cbfb$^{+/+}$		*Cbfb*$^{rss/+}$		*Cbfb*$^{+/-}$		*Cbfb*$^{rss/rss}$		*Cbfb*$^{rss/-}$	
Cell type/marker	Mean ± SD	n	Mean ± SD	n	Mean ± SD	n	Mean ± SD	n	Mean ± SD	n
CD45$^+$ splenocytes*†	25.6 ± 2.4	21	24.0 ± 0.5	4	18.8 ± 2.7§	10	21.1 ± 3.9	4	16.3 ± 2.5‖	21
CD45$^+$ Gr-1$^+$ Mac-1$^+$ monocytes/granulocytes*‡	56.5 ± 2.7	4	61.0 ± 3.5	9	ND		29.4 ± 3.4‖	6	15.0 ± 2.5§	4
Ter119$^+$ erythroid cells*†	50.0 ± 4.5	10	52.3 ± 3.9	14	ND		39.0 ± 8.1	7	58.5 ± 8.9	5
CD19$^+$ B cells*†	3.0 ± 0.5	13	3.0 ± 0.4	3	3.0 ± 0.5	9	3.5 ± 0.5	3	3.6 ± 1.1	14
Thymocytes										
CD4$^+$ CD8$^+$ DP†	49.0 ± 7.0	25	38.2 ± 4.0	9	36.5 ± 7.0	5	31.7 ± 9.0§	7	4.3 ± 3.3‖	25
CD4$^+$ CD8$^-$†	5.4 ± 0.4	40	6.4 ± 0.6	22	8.5 ± 1.7§	5	18.3 ± 2.2‖	7	7.3 ± 4.0	25
CD4$^-$ CD8$^+$†	3.6 ± 0.7	25	4.7 ± 0.3	9	3.2 ± 1.3	5	2.1 ± 0.5	7	0.8 ± 0.4‖	25
Spleen cellularity	1.6 ± 0.2 × 10^6	7	1.5 ± 0.1 × 10^6	5	1.1 ± 0.1 × 10^6	8	5.3 ± 0.3 × 10^5§	3	4.8 ± 0.8 × 10^5§	6
Thymus cellularity	6.0 ± 0.5 × 10^6	12	4.0 ± 0.1 × 10^6	4	4.0 ± 0.5 × 10^6	6	8.3 ± 0.3 × 10^5‖	6	4.9 ± 1.2 × 10^5‖	14

ND indicates not done.
*Spleen.
†Expressed as percentage of all spleen or thymus cells expressing the antigen.
‡Cells gated for CD45 expression were analyzed for Gr-1 and Mac-1 expression. Values represent the percentage of CD45$^+$ cells that were also Gr-1$^+$Mac-1$^+$.
§Significantly different from *Cbfb*$^{+/+}$ at $P < .001$ by unpaired 2-tailed Student *t* test.
‖Significantly different from *Cbfb*$^{+/+}$ at $P < .001$.

of a marked developmental impairment of *Cbfb*$^{rss/-}$ progenitors at the ETP to DN2 transition, causing a profound competitive advantage for the small number of Ly5.1$^+$ competitor cells. In some animals, including *rss/−* (1), we also observed decreased FL donor-cell contribution to the ETP population, suggesting an even earlier impairment in the generation of ETPs or in their subsequent expansion. In the second group of recipient mice, represented by *rss/−* (2), *Cbfb*$^{rss/-}$ donor cells contributed to the ETP and DN2 populations, but less well to DN3 thymocytes, indicating a partial block at the DN2 to DN3 transition. Therefore *Cbfb*$^{rss/-}$ cells exhibit additive partial impairments at consecutive stages of early thymocyte development—in the generation/expansion of ETPs, in the differentiation of ETPs to DN2 cells, and in the differentiation of DN2 to DN3 cells. The overall result of these defects is a complete or near-complete block in the generation of mature thymocytes. We also saw similar, variable partial blocks at these early differentiation steps in 17.5-dpc fetuses (not shown).

Cbfb$^{rss/rss}$ thymocytes inefficiently extinguish CD4 expression

The increase in CD4 expression we observed in immature thymocytes in 17.5-dpc *Cbfb*$^{rss/rss}$ fetuses (Figure 4H; Table 2) was recapitulated in the transplant recipients (Figure 6B-D). The donor-derived CD4$^-$CD8$^-$ DN population of thymocytes was shifted upward in the direction of higher CD4 expression (Figure 6B, arrows in lower panels). *Cbfb*$^{rss/rss}$ FL cells also contributed to 3-fold fewer immature single-positive (ISP) cells (not shown). We examined CD4 expression in all 4 DN subsets to determine when the up-regulation of CD4 expression occurred. We excluded all lineage-positive cells with the exception of CD4$^+$ cells, and separated the FL donor-derived (Ly5.2$^+$) Lin$^-$ cells into ETP, DN2, DN3, and DN4 populations based on c-kit and CD25 expression (Figure 6D, scatterplots). CD4 expression in the donor-derived DN3 and DN4 thymocyte populations was higher in recipients reconstituted with *Cbfb*$^{rss/rss}$ FL cells compared with *Cbfb*$^{+/+}$ cells (Figure 6D, histograms), suggesting that Runx1-CBFβ normally represses CD4 expression at these 2 stages. We did not, however, observe a similar depression of CD4 in mature CD8$^+$ cells (Figure 6D). Runx3 and Runx1 together repress CD4 expression in CD8$^+$ cells,[7,8] but apparently the CBFβ levels present in *Cbfb*$^{rss/rss}$ cells are sufficient to support Runx3 and Runx1 function at this stage of T-cell differentiation.

Discussion

Homozygous deletion of *Cbfb* in the embryo results in the absence of all definitive blood-cell lineages.[15,16] Here, we show with a hypomorphic *Cbfb* allelic series that once HSCs emerge there is a continued requirement for CBFβ in T-cell, megakaryocyte, granulocyte, and bone development. Reduced CBFβ levels also increased the numbers of committed hematopoietic progenitors and phenotypic KSL cells. As the alterations in progenitors and megakaryocytes were reminiscent of those reported for Runx1 haploinsufficiency and deficiency in the adult,[5,6,19] we have focused our discussion on the perturbations that are unique to the *Cbfb* allelic series of mice, as these define threshold levels of CBFβ necessary to sustain the development of several cell lineages, and reveal pathways for which the combined activity of 2 or more Runx proteins is required.

Redundant functions for Runx proteins in granulocyte development

Deficiencies in granulocyte development were not observed upon conditional deletion of Runx1 in the adult using Mx1-Cre,[5,6,32] nor were they described in Runx2- or Runx3-deficient mice.[14,33] Furthermore, no congenital neutropenias have been mapped to core-binding factor genes. Therefore the block before the promyelocyte stage caused by reductions in CBFβ levels suggests that the Runx proteins provide redundant functions in granulopoiesis during fetal development. In retrospect, this was predictable given the many examples of granulocyte defects in mice or cells expressing dominant-negative CBF fusion proteins. For example, expression of the *CBFB/MYH11* fusion gene from the myeloid-specific *hMRP8* promoter in mice increased the percentage of immature neutrophils in the bone marrow.[34] Mice repopulated with bone marrow cells in which a *CBFB/MYH11* allele was conditionally activated in the adult exhibited a donor-derived multilineage block in hematopoiesis involving all lineage-positive myeloid and lymphoid cells (B220$^+$CD3$^+$Mac-1$^+$Gr-1$^+$).[21] Overexpression and ectopic expression of AML1/ETO has also been shown to block myeloid-cell differentiation in multiple cell lines and in primary bone marrow cells.[35] It is unclear which Runx proteins are involved

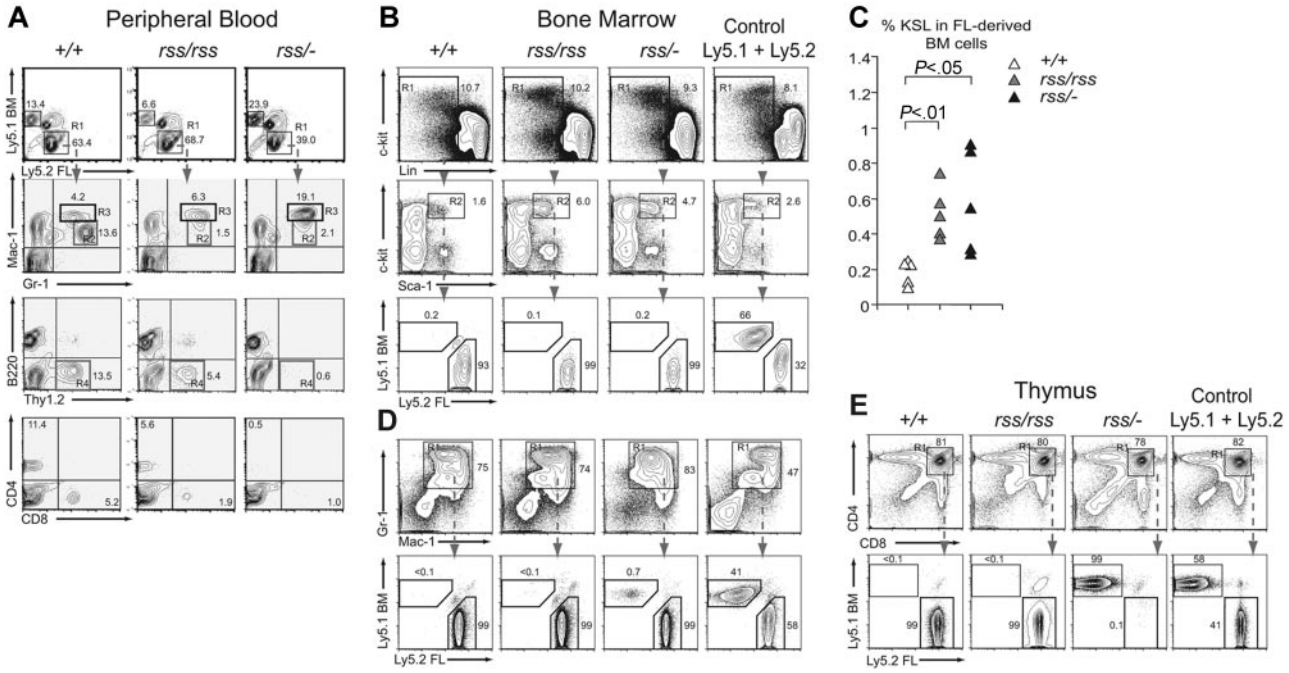

Figure 5. Defects in T cells and granulocytes are cell autonomous. (A) Top panels show contribution of donor FL cells (Ly5.2$^+$) and competitor BM (Ly5.1$^+$) to peripheral blood 4 months after transplantation. The contribution of FL donor cells (R1 gate) to granulocytes (Gr-1$^+$ and Mac-1$^+$), B (B220$^+$) and T (Thy1.2$^+$) lymphocytes, and CD4$^+$ and CD8$^+$ T cells is shown in panels below. The R2 and R3 gates surround Gr-1^{hi}Mac-1^{lo} and Gr-1^{hi}Mac-1^{hi} populations, respectively. Cells in the R4 gate are FL-derived Thy1.2$^+$ T cells, which are absent in mice reconstituted with *Cbfb*$^{rss/-}$ cells. Equivalent contribution to B220$^+$ B cells is seen with all 3 *Cbfb* genotypes. $n_{+/+} = 9$, $n_{rss/rss} = 9$, and $n_{rss/-} = 11$; shown are representative recipients. (B) Relative contribution of *Cbfb*$^{+/+}$, *Cbfb*$^{rss/rss}$, and *Cbfb*$^{rss/-}$ FL cells versus BM competitor cells to the KSL population in the BM of recipient mice, analyzed 12 months after transplantation. A mixture of Ly5.1$^+$ and Ly5.2$^+$ BM is shown as a control. Cells in gated regions (R1, R2) are analyzed in the plots below. Note the overwhelming contribution of FL cells (Ly5.2$^+$) from all 3 *Cbfb* genotypes to the KSL population. (C) Percentage of c-Kit$^+$Sca-1$^+$Lin$^-$ (KSL) donor-derived progenitors in bone marrow of mice that received a transplant of *Cbfb*$^{+/+}$, *Cbfb*$^{rss/rss}$, or *Cbfb*$^{rss/-}$ FL cells. (D) Contribution of FL donor and BM competitor cells to Gr-1$^+$Mac-1$^+$ BM cells. (E) Contribution of *Cbfb*$^{+/+}$, *Cbfb*$^{rss/rss}$, and *Cbfb*$^{rss/-}$ FL cells to CD4$^+$CD8$^+$ cells in the thymus of transplant recipients. Note that although the KSL and Gr-1$^+$Mac-1$^+$ populations in mice reconstituted with *Cbfb*$^{rss/-}$ FL cells are predominantly donor derived (B,D), CD4$^+$CD8$^+$ cells are derived almost entirely from the competitor BM.

in granulocyte differentiation, as only Runx1 expression has been extensively characterized in this lineage. Both Runx1 and CBFβ are expressed in functional CFU-GEMM and CFU-GM progenitors, and in mature granulocytes.[36-38] Immunohistochemical analyses of fetal liver suggested Runx3 is expressed in myeloid precursors,[39] but Runx3 protein was not detected in mature neutrophils in the adult.[14] Runx2 expression in the granulocyte lineage has not been reported.

Granulocyte development requires the activity of multiple transcription factors including C/EBPα, C/EBPϵ, PU.1, c-Myb, retinoic acid receptors, and Gfi-1.[22] Granulocytes in C/EBPα-deficient mice are blocked at the myeloblast stage, and lack expression of the GCSFR, which is a C/EBPα target.[26] Neither C/EBPα nor GCSFR levels were significantly altered in *Cbfb*$^{rss/-}$ Gr-1$^+$ cells, indicating that C/EBPα is upstream of the CBFs. However embryonic stem cells heterozygous for the dominant-negative *CBFB/MYH11* allele contributed only to erythrocytes, and not to any Mac-1$^+$/Gr-1$^+$ cells in chimeric mice,[40] indicating that further reduction of functional CBFβ levels causes even earlier blocks in myeloid development upstream of C/EBPα. Deletion of PU.1 in either the fetus or adult results in an absence of common myeloid and granulocyte monocyte progenitors, and a complete absence of mature neutrophils.[41,42] This also places PU.1 before CBFβ in granulocyte development, although the decrease in PU.1 levels in *Cbfb*$^{rss/-}$ cells suggests PU.1 is a direct or indirect CBFβ target at later stages. C/EBPϵ is required later than CBFβ, after the promyelocyte stage of development,[43] and its levels were significantly reduced in *Cbfb*$^{rss/-}$ cells. C/EBPϵ is required for the expression of secondary and tertiary granule proteins,[24] thus reduced lactoferrin and gelatinase B expression in *Cbfb*$^{rss/-}$ cells could be caused by decreased C/EBPϵ levels. The defects in *Cbfb*$^{rss/-}$ fetal granulocytes most closely resemble those reported in Gfi-1–deficient mice,[44] but the block appears to be somewhat earlier since the primary granule protein neutrophil elastase was expressed in Gfi-1–deficient cells, but not in *Cbfb*$^{rss/-}$ cells. Granulocyte development from *Cbfb*$^{rss/-}$ cells in transplant recipients was much less perturbed than in the fetus, suggesting that the sensitivity to low CBFβ levels is diminished in the adult.

Reduced CBFβ dosage affects the development of T cells more than B cells

Perhaps the most interesting differences seen upon reduced CBFβ dosage compared with Runx1 deficiency were in the B- and T-cell lineages. Runx1-deficient bone marrow was unable to contribute to B220$^+$ cells upon transplantation into recipient mice,[5,6] and one group reported reduced numbers of common lymphoid progenitors (CLPs).[5] In contrast, we observed that a 6- to 7-fold reduction in CBFβ levels caused only a modest, 2- to 3-fold reduction of B-cell numbers in the fetal spleen, and no obvious effect on the ability of FL cells to contribute to the pool of B220$^+$ cells in reconstituted mice. Thus, although B-cell development requires Runx1, relatively low levels of CBFβ are adequate to support Runx1 function and to maintain normal numbers of B cells in adult mice. Conditional rescues of CBFβ deficiency using either Gata1- or Tek-driven CBFβ transgenes, neither of which is expressed in B cells, were unable to support the normal production of B220$^+$

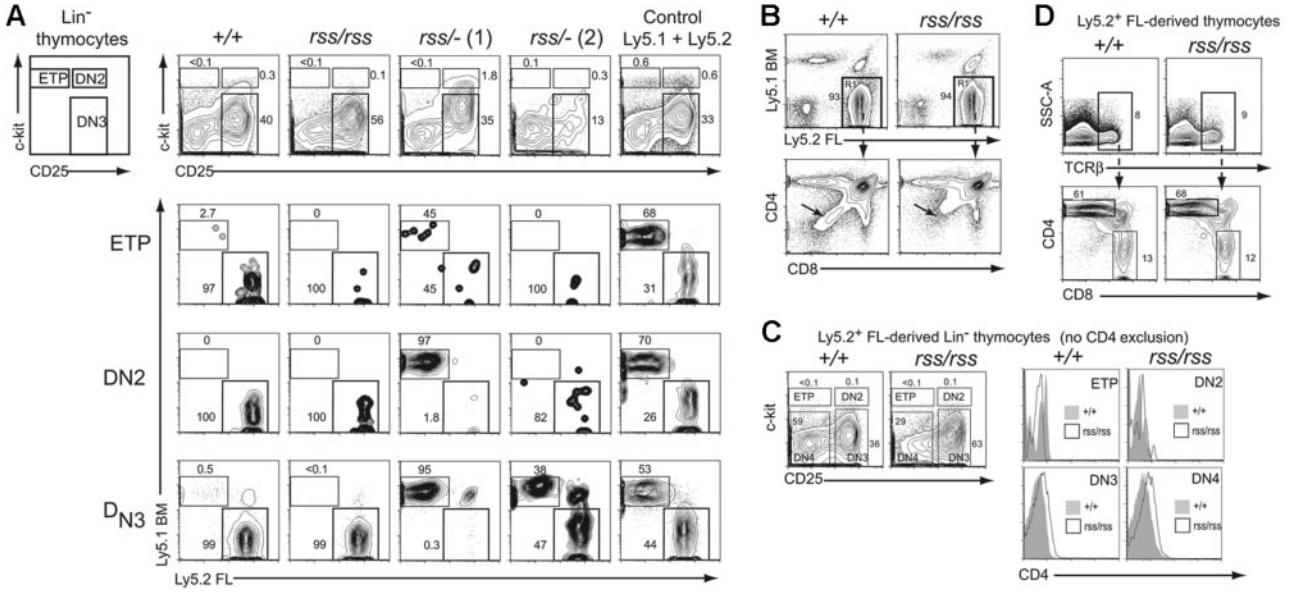

Figure 6. Characterization of cell-autonomous T-cell developmental defects. (A) Lin⁻ thymocytes from transplant recipients were separated based on c-kit and CD25 expression into ETP (c-kit⁺ CD25⁻), DN2 (c-kit⁺ CD25⁺), and DN3 (c-kit⁻ CD25⁺) populations (top panels), and each population was analyzed for donor FL and BM-competitor–cell contribution in the 3 panels below. Two independent recipients of transplanted *Cbfb*$^{rss/-}$ FL cells are shown. Of the 9 transplant recipients of *Cbfb*$^{rss/-}$ FL cells, 6 resembled the pattern seen with *rss/–* (1) and 3 resembled *rss/–* (2). (B) CD4 expression is derepressed in *Cbfb*$^{rss/rss}$ FL cells (bottom panels, arrows). (C) CD4 expression is up-regulated in the DN3 and DN4 populations. c-kit and CD25 were used to define the ETP, DN2, DN3, and DN4 populations from donor-derived Lin⁻ cells (scatterplots). Antibodies in the lineage-specific cocktail did not include CD4. Each population was analyzed for CD4 expression (histograms). (D) CD4 is not derepressed in *Cbfb*$^{rss/rss}$ CD8 SP thymocytes. TCRβ^{hi} cells were analyzed for CD4 and CD8 expression in the panels below.

cells,[17,45] indicating that CBFβ is, however, required for B-cell development.

In contrast to the relative insensitivity of B cells, T-cell development was exquisitely sensitive to an incremental reduction in CBFβ dosage. A decrease in CBFβ levels to 30% of normal in *Cbfb*$^{rss/rss}$ cells led to a modest impairment in the efficiency of αβ and γδ T-cell development. In addition, we observed a subtle defect in CD4 silencing among immature thymocytes and a decrease in the number of ISP thymocytes that was likely related to premature CD4 up-regulation in these cells. These changes were reminiscent of CD4 derepression observed in the absence of Runx1 activity and suggested that relatively high CBFβ levels (> 30% of normal) were required to sustain Runx1-mediated silencing of the *Cd4* locus in DN thymocytes. Despite these abnormalities, the overall efficiency of T-cell development from *Cbfb*$^{rss/rss}$ cells was well preserved even in a competitive setting in the adult environment. However, a further reduction in CBFβ levels to 15% of normal in *Cbfb*$^{rss/-}$ cells dramatically impaired both fetal and adult thymopoiesis, as evidenced by the near-complete disappearance of mature thymocytes. These findings define a critical threshold of CBFβ dosage (between 15% and 30% of normal levels) that is absolutely required to sustain T-cell development.

The impaired progression of *Cbfb*$^{rss/-}$ T-lineage progenitors could be mapped precisely to the earliest stages of T-cell development in the thymus. Indeed, a competitive disadvantage of these cells was already apparent upstream of DN3 thymocytes within the ETP and DN2 T-cell progenitor populations. Although there was some variation in the precise differentiation block in individual mice, possibly related to epigenetic differences in residual CBFβ concentration or in the relative fitness of competitor cells, the predominant pattern was a very proximal block that was already apparent in the ETP population or in its immediate progeny. ETPs are a subset of DN1 thymocytes that were identified as the earliest and most potent T-lineage progenitors in the adult thymus.[30,46,47] Recent evidence indicates that the generation and subsequent differentiation of ETPs requires ongoing delivery of Notch signals.[48-50] Our findings suggest the existence of a concomitant continuous requirement for core-binding factor activity during differentiation of ETPs to DN2 and DN3 thymocytes. An important goal of future research will be to define the specific targets of core-binding factors during early T-lineage differentiation, as well as their potential interactions with other critical molecular pathways, such as Notch signaling, or the GATA3 and E2A transcription factors (reviewed in Rothenberg and Taghon[51]). Of note, we observed no accumulation of *Cbfb*$^{rss/-}$ intrathymic B cells, suggesting that reduced levels of CBFβ did not impair the sensitivity of progenitors to Notch signaling, at least in terms of Notch-mediated repression of B-cell development.

A reduction of CBFβ levels to 15% of normal in *Cbfb*$^{rss/-}$ cells caused an apparently earlier T-lineage developmental defect than described in adult mice lacking Runx1.[5,6] In Runx1-deficient mice, the bulk of DN2 thymocytes appeared preserved, and the most significant differentiation block was described at the DN2/DN3 transition, even in the presence of wild-type competitors in mixed bone marrow chimeras. In contrast, T-cell development was impaired upstream of DN2 thymocytes in the majority of mice we examined. All 3 Runx proteins and CBFβ were detected in DN thymocytes.[8,36-38,52] These results suggest that CBFβ might partner not only with Runx1, but perhaps also with Runx2 or Runx3 during early stages of T-cell development.

Two thresholds for CBFβ levels in bone development

The *Cbfb* allelic series convincingly shows that 3-fold reductions in CBFβ levels are adequate to cause obvious defects in bone formation, while 6- to 7-fold reductions do not allow ossification. Thus, as in the case of T-cell development, 2 important thresholds for CBFβ levels in bone formation could be documented. A

1.2-megabase deletion encompassing *CBFB* was recently described in a patient with mild skeletal impairments that included wide fontanelles and delayed chondrocyte maturation, and large cranial sutures were seen in 7 of 8 cases with interstitial 16q deletions.[53] Although other genes could be deleted in that interval, it suggests that even *CBFB* haploinsufficiency could possibly contribute to mild skeletal abnormalities in some individuals.

Finally, the *Cbfb* allelic series provides an important benchmark against which the effect of the dominant-negative *CBFB/MYH11* allele can be measured. Mice heterozygous for a *CBFB/MYH11* knock-in allele die at midgestation with an impairment in definitive hematopoiesis much more severe than that seen in $Cbfb^{rss/-}$ fetuses.[54] Thus, the reduction in the functional CBFβ dosage caused by the presence of the *CBFB/MYH11* allele exceeds 6- to 7-fold.

Acknowledgments

This work was supported by RO1 CA75611 (N.A.S.), RO1 AI047833 (W.S.P.), the Damon Runyon Cancer Research Foundation DRG-102-05 (I.M.), and T32 AR07576 (J.G.). Flow cytometry, biostatistics, and the transgenic mouse facility were supported in part by the Core Grant of the Norris Cotton Cancer Center (CA 23108).

We thank Steve Fiering for the *Tg(CMV-Cre)* mice, and Caroline Speck, Torrey Gallagher, Diane Church, Brandon Zeigler, Gary Ward, Eugene Demidenko, Zhao Chen, Véronique Lefebvre, Bogdan Dumitriu, Ramesh Shivdasani, and Alice Givan for their advice and/or assistance.

Authorship

Contribution: L.T. performed the experiments described in Figures 2C, 3A-B, and 4B-F,H, and Table 1; Z.L. performed the experiments described in Figures 1 and 2A-B; Y.G. performed the experiments described in Figure 4H; J.G. performed the experiments described in Figure 4G; M.E.S. performed the experiments described in Figures 3C and 4A; D.S. and P.K. assisted in the interpretation of Figure 4E; W.S.P. assisted in the paper preparation; I.M. assisted in the design of the experiments, performed the work described in Figures 5-6, and helped write the paper; N.A.S. participated in the design and interpretation of the experiments and writing of the paper.

Conflict-of-interest disclosure: The authors declare no competing financial interests.

Correspondence: Ivan Maillard, Division of Hematology-Oncology, University of Pennsylvania School of Medicine, Philadelphia, PA 19104-6160; e-mail: ivan.maillard@uphs.upenn.edu; or Nancy A. Speck, Department of Biochemistry, Dartmouth Medical School, Hanover, NH 03755; e-mail: nancy.speck@dartmouth.edu.

References

1. Besmer P. The kit ligand encoded at the murine Steel locus: a pleiotropic growth and differentiation factor. Curr Opin Cell Biol. 1991;3:939-946.
2. Bernstein A, Forrester L, Reith AD, Dubreuil P, Rottapel R. The murine W/c-kit and Steel loci and the control of hematopoiesis. Semin Hematol. 1991;28:138-142.
3. Huizinga JD, Thuneberg L, Kluppel M, Malysz J, Mikkelsen HB, Bernstein A. W/kit gene required for interstitial cells of Cajal and for intestinal pacemaker activity. Nature. 1995;373:347-349.
4. Cai Z, de Bruijn MFTR, Ma X, et al. Haploinsufficiency of AML1/CBFA2 affects the embryonic generation of mouse hematopoietic stem cells. Immunity. 2000;13:423-431.
5. Growney JD, Shigematsu H, Li Z, et al. Loss of Runx1 perturbs adult hematopoiesis and is associated with a myeloproliferative phenotype. Blood. 2005;106:494-504.
6. Ichikawa M, Asai T, Saito T, et al. AML-1 is required for megakaryocytic maturation and lymphocytic differentiation, but not for maintenance of hematopoietic stem cells in adult hematopoiesis. Nat Med. 2004;10:299-304.
7. Taniuchi I, Osato M, Egawa T, et al. Differential requirements for Runx proteins in CD4 repression and epigenetic silencing during T lymphocyte development. Cell. 2002;111:621-633.
8. Woolf E, Xiao C, Fainaru O, et al. Runx3 and Runx1 are required for CD8 T cell development during thymopoiesis. Proc Natl Acad Sci U S A. 2003;100:7731-7736.
9. Komori T, Yagi H, Nomura S, et al. Targeted disruption of Cbfa1 results in a complete lack of bone formation owing to maturational arrest of osteoblasts. Cell. 1997;89:755-764.
10. Otto F, Thornell AP, Crompton T, et al. Cbfa1, a candidate gene for Cleidocranial dysplasia syndrome, is essential for osteoblast differentiation and bone development. Cell. 1997;89:765-772.
11. Inada M, Yasui T, Nomura S, et al. Maturational disturbance of chondrocytes in Cbfa1-deficient mice. Dev Dyn. 1999;214:279-290.
12. Kim I, Otto F, Zabel B, Mundlos S. Regulation of chondrocyte differentiation by Cbfa1. Mech Dev. 1999;80:159-170.
13. Yoshida CA, Yamamoto H, Fujita T, et al. Runx2 and Runx3 are essential for chondrocyte maturation, and Runx2 regulates limb growth through induction of Indian hedgehog. Genes Dev. 2004; 18:952-963.
14. Fainaru O, Woolf E, Lotem J, et al. Runx3 regulates mouse TGF-beta-mediated dendritic cell function and its absence results in airway inflammation. EMBO J. 2004;23:969-979.
15. Sasaki K, Yagi H, Bronson RT, et al. Absence of fetal liver hematopoiesis in mice deficient in transcriptional coactivator core binding factor beta. Proc Natl Acad Sci U S A. 1996;93:12359-12363.
16. Wang Q, Stacy T, Miller JD, et al. The CBFβ subunit is essential for CBFα2 (AML1) function in vivo. Cell. 1996;87:697-708.
17. Miller J, Horner A, Stacy T, et al. The core-binding factor β subunit is required for bone formation and hematopoietic maturation. Nat Genet. 2002; 32:645-649.
18. Shivdasani RA, Fielder P, Keller GA, Orkin SH, de Sauvage FJ. Regulation of the serum concentration of thrombopoietin in thrombocytopenic NF-E2 knockout mice. Blood. 1997;90:1821-1827.
19. Sun W, Downing JR. Haploinsufficiency of AML1 results in a decrease in the number of LTR-HSCs while simultaneously inducing an increase in more mature progenitors. Blood. 2004;104:3565-3572.
20. Song W-J, Sullivan MG, Legare RD, et al. Haploinsufficiency of CBFA2 (AML1) causes familial thrombocytopenia with propensity to develop acute myelogenous leukamia (FPD/AML). Nat Genet. 1999;23:166-175.
21. Kuo YH, Landrette SF, Heilman SA, et al. Cbf beta-SMMHC induces distinct abnormal myeloid progenitors able to develop acute myeloid leukemia. Cancer Cell. 2006;9:57-68.
22. Friedman AD. Transcriptional regulation of granulocyte and monocyte development. Oncogene. 2002;21:3377-3390.
23. Lausen J, Liu S, Fliegauf M, Lubbert M, Werner MH. ELA2 is regulated by hematopoietic transcription factors, but not repressed by AML1-ETO. Oncogene. 2006;25:1349-1357.
24. Lekstrom-Himes J, Xanthopoulos KG. CCAAT/enhancer binding protein epsilon is critical for effective neutrophil-mediated response to inflammatory challenge. Blood. 1999;93:3096-3105.
25. Verbeek W, Lekstrom-Himes J, Park DJ, et al. Myeloid transcription factor C/EBPepsilon is involved in the positive regulation of lactoferrin gene expression in neutrophils. Blood. 1999;94: 3141-3150.
26. Zhang DE, Zhang P, Wang ND, Hetherington CJ, Darlington GJ, Tenen DG. Absence of granulocyte colony-stimulating factor signaling and neutrophil development in CCAAT enhancer binding protein alpha-deficient mice. Proc Natl Acad Sci U S A. 1997;94:569-574.
27. Radtke F, Wilson A, Stark G, et al. Deficient T cell fate specification in mice with an induced inactivation of Notch1. Immunity. 1999;10:547-558.
28. Wilson A, MacDonald HR, Radtke F. Notch 1-deficient common lymphoid precursors adopt a B cell fate in the thymus. J Exp Med. 2001;194:1003-1012.
29. Rebel VI, Miller CL, Eaves CJ, Lansdorp PM. The repopulation potential of fetal liver hematopoietic stem cells in mice exceeds that of their liver adult bone marrow counterparts. Blood. 1996;87:3500-3507.
30. Allman D, Sambandam A, Kim S, et al. Thymopoiesis independent of common lymphoid progenitors. Nat Immunol. 2003;4:168-174.
31. Schwarz BA, Bhandoola A. Circulating hematopoietic progenitors with T lineage potential. Nat Immunol. 2004;5:953-960.
32. Putz G, Rosner A, Nuesslein I, Schmitz N, Buchholz F. AML1 deletion in adult mice causes

splenomegaly and lymphomas. Oncogene. 2006; 25:929-939.

33. Deguchi K, Yagi H, Inada M, Yoshizaki K, Kishimoto T, Komori T. Excessive extramedullary hematopoiesis in Cbfa1-deficient mice with a congenital lack of bone marrow. Biochem Biophys Res Commun. 1999;255:352-359.
34. Kogan SC, Lagasse E, Atwater S, et al. The PEBP2βMYH11 fusion created by Inv(16)(p13; q22) in myeloid leukemia impairs neutrophil maturation and contributes to granulocytic dysplasia. Proc Natl Acad Sci U S A. 1998;95:11863-11868.
35. Peterson LF, Zhang DE. The 8;21 translocation in leukemogenesis. Oncogene. 2004;23:4255-4262.
36. Kundu M, Chen A, Anderson S, et al. Role of Cbfb in hematopoiesis and perturbations resulting from expression of the leukemogenic fusion gene Cbfb-MYH11. Blood. 2002;100:2449-2456.
37. Lorsbach RB, Moore J, Ang SO, Sun W, Lenny N, Downing JR. Role of Runx1 in adult hematopoiesis: analysis of Runx1-IRES-GFP knock-in mice reveals differential lineage expression. Blood. 2004;103:2522-2529.
38. North TE, de Bruijn MFTR, Stacy T, et al. Runx1 expression marks long-term repopulating hematopoietic stem cells in the midgestation mouse embryo. Immunity. 2002;16:661-672.
39. Levanon D, Brenner O, Negreanu V, et al. Spatial and temporal expression pattern of Runx3 (Aml2) and Runx1 (Aml1) indicates non-redundant functions during mouse embryogenesis. Mech Dev. 2001;109:413-417.
40. Castilla LH, Garrett L, Adya N, et al. Chromosome 16 inversion-generated fusion gene Cbfb-MYH11 blocks myeloid differentiation and predisposes mice to acute myelomonocytic leukemia. Nat Genet. 1999;23:144-146.
41. Iwasaki H, Somoza C, Shigematsu H, et al. Distinctive and indispensable roles of PU.1 in maintenance of hematopoietic stem cells and their differentiation. Blood. 2005;106:1590-1600.
42. Kim HG, de Guzman CG, Swindle CS, et al. The ETS family transcription factor PU.1 is necessary for the maintenance of fetal liver hematopoietic stem cells. Blood. 2004;104:3894-3900.
43. Yamanaka R, Barlow C, Lekstrom-Himes J, et al. Impaired granulopoiesis, myelodysplasia, and early lethality in CCAAT/enhancer binding protein epsilon-deficient mice. Proc Natl Acad Sci U S A. 1997;94:13187-13192.
44. Hock H, Hamblen MJ, Rooke HM, et al. Intrinsic requirement for zinc finger transcription factor Gfi-1 in neutrophil differentiation. Immunity. 2003; 18:109-120.
45. Yoshida CA, Furuichi T, Fujita T, et al. Core-binding factor β interacts with Runx2 and is required for skeletal development. Nat Genet. 2002;32: 633-638.
46. Porritt HE, Rumfelt LL, Tabrizifard S, Schmitt TM, Zuniga-Pflucker JC, Petrie HT. Heterogeneity among DN1 prothymocytes reveals multiple progenitors with different capacities to generate T cell and non-T cell lineages. Immunity. 2004;20: 735-745.
47. Balciunaite G, Ceredig R, Rolink AG. The earliest subpopulation of mouse thymocytes contains potent T, significant macrophage, and natural killer cell but no B-lymphocyte potential. Blood. 2005; 105:1930-1936.
48. Schmitt TM, Ciofani M, Petrie HT, Zuniga-Pflucker JC. Maintenance of T cell specification and differentiation requires recurrent notch receptor-ligand interactions. J Exp Med. 2004;200:469-479.
49. Tan JB, Visan I, Yuan JS, Guidos CJ. Requirement for Notch1 signals at sequential early stages of intrathymic T cell development. Nat Immunol. 2005;6:671-679.
50. Sambandam A, Maillard I, Zediak VP, et al. Notch signaling controls the generation and differentiation of early T lineage progenitors. Nat Immunol. 2005;6:663-670.
51. Rothenberg EV, Taghon T. Molecular genetics of T cell development. Annu Rev Immunol. 2005;23: 601-649.
52. Vaillant F, Blyth K, Terry A, et al. A full-length Cbfa1 gene product perturbs T-cell development and promotes lymphomagenesis in synergy with myc. Oncogene. 1999;18:7124-7134.
53. Goto T, Aramaki M, Yoshihashi H, et al. Large fontanelles are a shared feature of haploinsufficiency of RUNX2 and its co-activator CBFB. Congenit Anom (Kyoto). 2004;44:225-229.
54. Castilla LH, Wijmenga C, Wang Q, et al. Defects of embryonic hematopoiesis and lethal hemorrhaging in mouse embryos heterozygous for a knocked-in leukemia gene CBFB-MYH11. Cell. 1996;87:687-696.

Erratum

In the commentary by Merlini entitled “Exciting new agents in multiple myeloma,” which appeared in the November 15, 2006, issue of *Blood* (Volume 108:3235-3236), there were 2 mistakes. The title should have read, “Exploiting new agents in multiple myeloma,” and the last sentence of the second paragraph should have read, “However, these agents can cause acute complications and disabling chronic adverse effects.”